Received: 1 October 2021 | Accepted: 25 October 2021

DOI: 10.1002/ces2.10111

International Journal of Ceramic Engineering & Science

RESEARCH ARTICLE

Corrosion of bauxite-based refractory castables and matrix components in hydrogen containing atmosphere

T. Leber | **S. Madeo** | **T. Tonnesen** | **R. Telle**

Institute of Mineral Engineering, RWTH Aachen University, Aachen, Germany

Correspondence
Tim Leber, Chair of Ceramics, Institute of Mineral Engineering, RWTH Aachen University, Aachen, Germany.
Email: leber@ghi.rwth-aachen.de

Abstract

For the transformation to a CO_2 neutral industry, fuel of traditionally fossil-fired furnaces is substituted by the subsequently addition of hydrogen. In these studies, refractory components are identified for the corrosion of refractories in (highly) reducing atmospheres. A bauxite-based refractory castable is set up in diluted, 9Ar 1H_2, hydrogen atmosphere. Additionally, a focus is set on the behavior of a common matrix phase, anorthite.

Corrosion experiments up to 1500°C using a tube furnace with the mentioned atmosphere have been scheduled. Amount and phase stability due to different time and temperature coordinates have been examined by XRD. Furthermore, the microstructure and in particular the bonding phase was observed by means of SEM and EDS. Microstructural components undergoing reaction or loss are identified and explained in regards of complete and incomplete hydrogen combustion. Reduction of impurities such as iron oxides, phosphorus oxides, and titanium oxides are considered in detail.

KEYWORDS
gas corrosion, hydrogen, refractory castable

1 | INTRODUCTION

The change in combustion and reaction components for aggregates in the course of the conversion to a CO-neutral economy also confronts refractory linings with changed conditions. The atmosphere in the aggregates, such as direct reduction plants from the iron and steel industry, will consist of increased proportions of water vapor and hydrogen.[1,2]

This increase in hydrogen enables the reduction of the oxides that come into contact. This reaction follows the general reaction equation:

$$MeO_y + H_2\ (g) = MeO_{y-1}\ (s, g) + H_2O\ (g) \qquad (1)$$

The so formed residual products may be gaseous under the given conditions. This will lead to mass loss via the gas flow. Additionally, this leads to the formation of water vapor, which, if the partial pressure is high enough, can then lead to the formation hydroxides, which in turn leads to a mass and volume increase.[3–7]

These reactions take place if a reduction in free enthalpy can be achieved. The difference in free enthalpy is considered as a function of the temperature and the equilibrium of the reaction partners involved. The application of these equations shows which reactions can take place under the given conditions. The height of the difference is an indicator for the priority of the reaction. Ellingham diagrams can be created from these

TABLE 1 Composition of the tested bauxite castable

	Bauxite castable [wt.-%]
Reactive alumina	12.5
Cement (Secar 71)	5
Kyanite	20
Bauxite 0–1 mm	27.5
Bauxite 1–3 mm	35
Deflocculent (FS65)	0.1
Water	7.5

TABLE 2 Formulation of the samples for anorthite synthesis

	Anorthite 1 [wt.-%]	Anorthite 2 [wt.-%]
Lime	4.8	11.8
Microsilica	42.9	23.8
Cement (Secar 71)	52.3	–
Sol (boehmite)	–	50.1
Reactive alumina	14.3	–
Water	70	–

relationships as a helpful basis for observation and prediction.[8]

Bauxite is a rock; it stems from laterite, which transforms into kaolin and further to bauxite. Hereby the amount of silica, iron, and kaolinite is reduced. Bauxite serves as the main source of alumina mostly in the form of the hydroxide gibbsite. Other accompanying compounds are also present, mainly of a siliceous nature. Remaining iron and/or titanium impurities are also present in bauxites. The chemical composition of bauxite varies and depends on the formation and regional characteristics of the ore.[9,10]

After preparation, calcination, and classification, bauxite can also be used directly for refractory applications. In this case, impurities influence the properties of the product accordingly.

2 | EXPERIMENTAL

First, the behavior of a bauxite-based refractory castable in a hydrogen containing atmosphere is considered. The composition is shown in Table 1. Calcium aluminate cement (CAC) is used as a binder. The matrix is composed of cement, reactive alumina, and kyanite aggregates. The largest proportion of the formulation is made up of bauxite, which represents the coarser part up to 3 mm.

The casting and densification of the castable takes place by means of vibration. The castable is then left in the moisture cabinet for 48 h to hydrate. After drying, the samples are fired at 1350°C for 6 h.

Furthermore, the behavior of a matrix component is also considered. In case of cement-bonded aluminosilicate castables, mineral phases form according to the associated ternary system of Al_2O_3–CaO–SiO_2, most prominently anorthite. In order to better observe their behavior, anorthite is synthesised from raw materials of the refractory domain. Two different formulations, Table 2, are chosen for this purpose.

In one recipe, liquid is added via a boehmite sol and in the other via water. Both mixtures are stoichiometrically designed for a complete conversion into anorthite. To achieve this, the formulations are kept at 1300°C for 24 h. The high addition of liquid in both recipes causes a high porosity, which leads to an increased surface area and thus to enhanced reactivity.

After sample preparation and initial characterization of the samples via weighing and apparent porosity, the actual testing takes place. For this purpose, samples are placed in a tube furnace (see Figure 1). The gas composition and the flow can be adjusted by means of a rotameter. In this series of tests, however, only diluted hydrogen-containing gas, 10 % hydrogen and 90 % argon, is used. The flow rate is set to 25 L/h to maintain the reducing atmosphere.

The materials were tested according to Table 3. Tests at 1100°C are oriented more toward the upper end of the

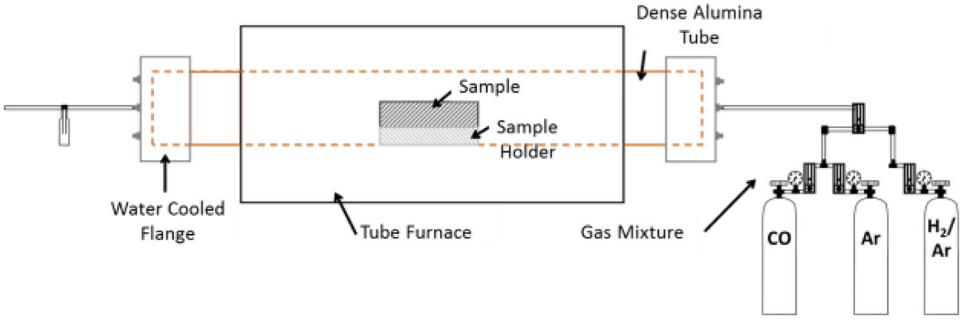

FIGURE 1 General experimental set-up of the tube furnace

TABLE 3 Overview of the trial types

Name	Material –	Temp. [°C]	Time [h]	Gasflow [L/h]
T0	Bauxite castable	1500	24	–
T1	Bauxite castable	1100	24	25
T2	Bauxite castable	1500	24	25
T3	Bauxite castable	1500	72	25
T4	Anorthite 1	1100	72	25
T5	Anorthite 2	1100	72	25

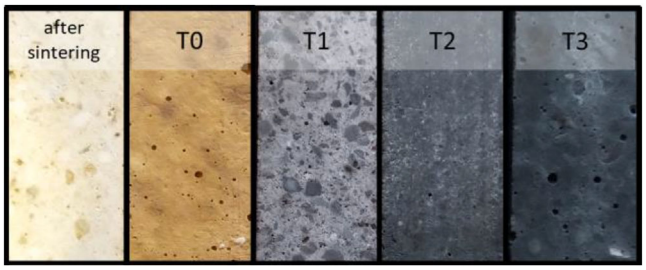

FIGURE 2 Surface of the bauxite castables samples after the corresponding experiments

operating conditions in direct reduction plants, whereas the increased temperatures of 1500°C are expected to lead to increased kinetics and thus more pronounced characteristics of corrosion. The influence of the test conditions on the samples is examined by means of mass control, chemical composition, phase composition, and microstructure. The chemical composition is determined by X-ray fluorescence (XRF), the system PW2404 from PANalytical (Netherlands) is used. The X-ray diffraction (XRD) for the mineral phase measurement is performed with a Bruker (USA) D8 Advance. Microstructural investigation is conducted via scanning electron microscopy (SEM) with a GeminiSEM 500 from Zeiss (Germany).

3 | RESULTS

After the tests, the castable sample shows visible macroscopical surface changes (Figure 2). These changes become more pronounced when the samples are kept at a higher temperature and for a longer duration. Since the samples were exposed to the same maximum temperature, T0 serves as a comparison to T2 and T3, while the sample after firing and can be compared to T1.

In general, the loss of mass (Table 4) is low, with a minimum loss of 0.06 % for T0 and a maximum loss of 0.67 % for T3. However, a tendency can be observed. The loss increases with higher temperature. A longer exposure time, T3, leads only to a small change, which is within the error margin of the shorter trial, T2. Mass control of the anorthite experiment series was unsuccessful as their respective strength is too low to minimize mass loss from handling and transport.

TABLE 4 Mass loss in the corresponding experiment types

Experiment	Mass loss [%]	Standard deviation
T0 (1500°C 24 h no gas)	0.06	0.03
T1 (1100°C 24 h)	0.35	0.05
T2 (1500°C 24 h)	0.60	0.17
T3 (1500°C 72 h)	0.67	0.19

TABLE 5 Chemical composition and loss on ignition of the bauxite castables

Component	T0 [wt.-%]	T1 [wt.-%]	T2 [wt.-%]
SiO_2	11.82	12.79	12.07
Al_2O_3	81.12	80.08	81.09
Fe_2O_3	1.89	1.84	1.89
TiO_2	2.50	2.42	2.51
CaO	1.67	1.88	1.64
P_2O_5	0.46	0.48	0.29
Others	0.54	0.51	0.51
LOI (1050°C)	0.07	−0.21	−0.40

TABLE 6 Mineral phase composition of the bauxite castables (main phase [+++], secondary phase [++])

Experiment	T0	T1	T2	T3
Corundum	+++	+++	+++	+++
Mullite	+++	+++	+++	+++
Anorthite	++	++	++	++

In order to observe which elements might be responsible for the previously considered mass loss, milled samples are observed by means of X-ray fluorescence analysis (Table 5). Here it is shown that the relative content of most compounds is stable over the test series.

The development in the case of P_2O_5 is noticeable. The basic content, T0, is about 0.5 wt.-% and also remains constant at T1. If the temperature is increased, T2, there is a decrease to 0.3 wt.-%. The loss on ignition (LOI) also shows the influence of the tests on the samples. A negative loss on ignition indicates an increase in mass, in this case, the oxidation of elements that were previously reduced in the experiment. This increase can be observed both at T1 and more pronounced at T2.

Table 6 shows the mineral phase composition of the sample at the respective experiment. It is noticeable that no large-scale change occurred in regard to the phase

TABLE 7 Mineral phase composition of the anorthite samples before and after testing (main phase [+++], secondary phase [++], traces [–])

	T4 initial	T4	T5 initial	T5
Anorthite	+++	+++	+++	+++
Cristobalite		–		–
CA_6		–		–
Gehlenite		–	++	++
Grossite			+	+
Corundum	–			
Wollastonite				–
Quartz	–	–		–

composition. The main phases in all cases are corundum and mullite. Mullite is a direct result of the transformation of kyanite, as well as components of the bauxite. Anorthite occurs as a secondary phase and is formed from the fine fractions after reaction with the cement.

The reason for the macroscopical changes in the samples could not be fully determined yet; therefore, a closer examination of the outer sample surface area is carried out by means of SEM/EDS.

In case of the test series with anorthite, more significant changes are measurable (Table 7). The cement-based anorthite, T4, initially contains anorthite, corundum, and quartz corresponding to the main phases and traces. Corundum stems from not fully converted reactive alumina. After the experiment, traces of CA_6, cristobalite, and gehlenite are also present.

In case of the second series, T5, the initial sample of the sol–gel formulation consists mainly of anorthite with traces of corundum and quartz. After exposure in the reducing gas stream, cristobalite, CA_6, gehlenite, and wollastonite are formed. As a consequence, the anorthite content decreases and corundum can no longer be detected.

To compare the development of the microstructural changes, a control sample from the test series T0 is examined. Figure 3 shows an overview; it can be noticed that iron oxides are dispersed in grains and matrix. Additionally, cracks and pores are present in the castable.

After exposure at 1100°C for 24 h, T1, no significant difference in comparison to samples after sintering is observed in the SEM. Although a surface change could be detected in the optical observation, it is not yet pronounced enough to be detect and quantified. Most of the iron and titanium oxides are still found in the grains and matrix of the sample.

The examination of the samples after the experiments T2 shows clear signs of change (Figure 4). Iron is no longer dispersed in the material system, but agglomerated on

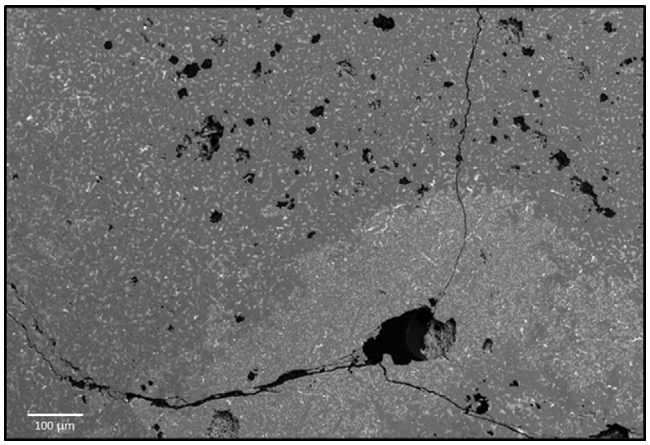

FIGURE 3 SEM micrograph overview of the bauxite castable from T0 (1500°C 24 h, no gas flow) with fine dispersed impurities such as Fe_2O_3

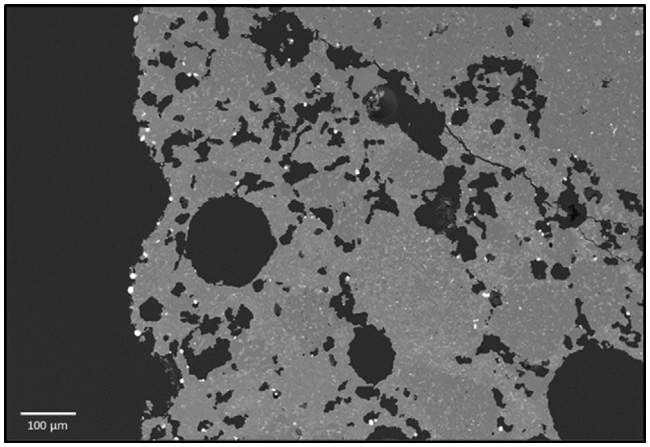

FIGURE 4 SEM micrograph overview of a bauxite castable after a T2 (1500°C 24 h) experiment with slightly agglomerated impurities

interfaces to the reducing gas, either in pore spaces or deposited on the sample surface.

At the outer surface of the sample (Figure 5), the beginning of layer formation can be observed. The measurements by means of EDS show that the deposits on the outer surface are mainly composed of iron. Some is present in metallic form (Figure 5, left). The EDS of the oxidized part (Figure 5, right) shows the presence of iron oxides as well as high amounts of phosphor.

Due to the high moveability, the hydrogen has permeated throughout the whole porous castable sample. This leads to the reduction of impurities, such as iron oxide and phosphor oxide, which then increases the moveability of these elements. They move along the concentration gradient toward the surrounding gas, especially toward the outer surface. During cooling, the reduced impurities are partially reoxidized.

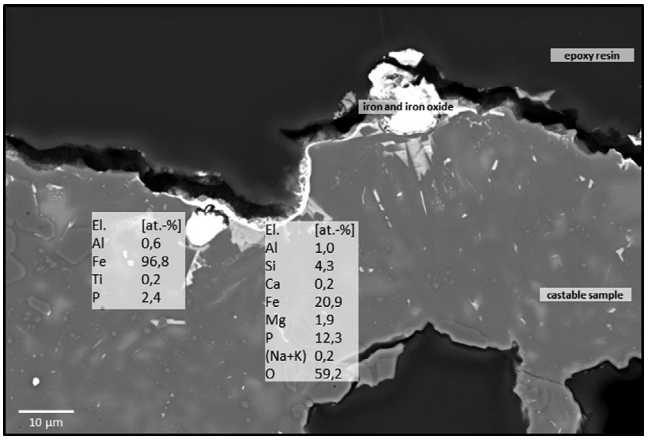

FIGURE 5 SEM micrograph of the outer sample surface after a T2 (1500°C 24 h) experiment with a clearly visible iron oxide layer

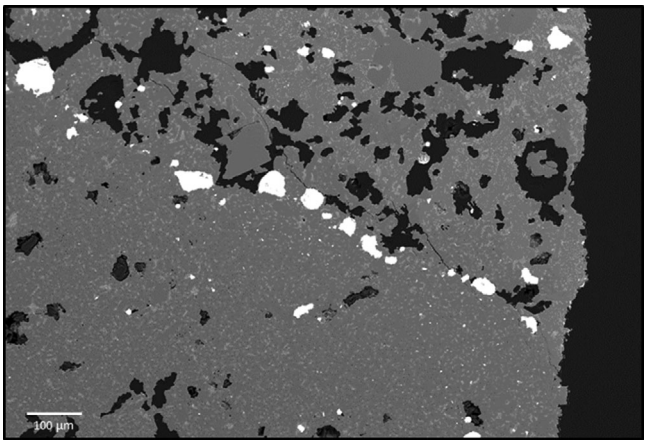

FIGURE 6 SEM micrograph overview of a bauxite castable after a T3 (1500°C 72 h) experiment with agglomerated impurities

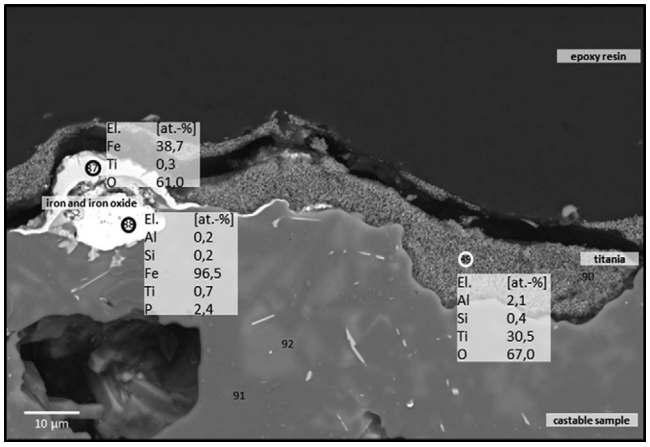

FIGURE 7 SEM micrograph of the outer sample surface after a T3 (1500°C 72 h) experiment with a clearly visible iron and titanium oxide layer

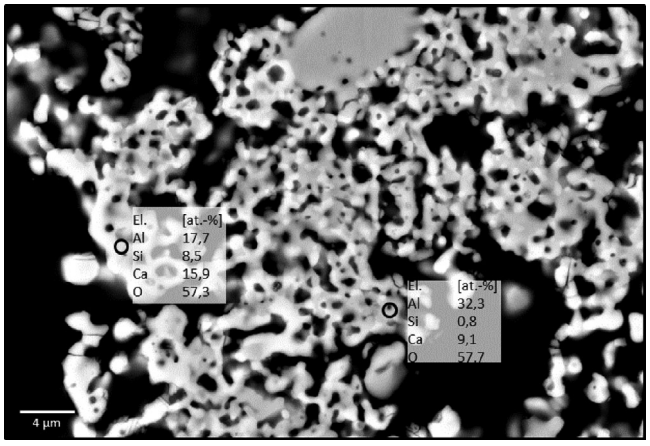

FIGURE 8 SEM micrograph of anorthite, based on cement, after T4 (1100°C 24 h)

If the sample is stored for a longer period, 72 h in the gas flow, the previously made observations are even more prominent. As it can be seen in Figure 6, the agglomerates are clearly larger with a diameter of approximately 75 μm compared to the ones from shorter trials with approximately 14 μm. As observed before, the agglomerates are formed at pores, partially connected by cracks.

When looking at the interface between sample and surroundings, changes in the accumulation can be seen (Figure 7). In addition to the previously observed layer of iron and iron oxides, there is now also a layer of titania present. This now forms the outer surface of the sample instead of the iron oxide layer. In regard to T2, the reaction and movement process in T3 encompasses titanium oxide in addition to iron and phosphor oxide.

In both recipes from the anorthite synthesis, a very porous network of anorthite is formed. In the case of the cement-based formulation after the test at 1100°C for 72 h, T4, the macroscopic structure of the sample does not differ. However, detailed examination of the finer parts reveals the presence of calciumaluminates (Figure 8).

In the case of the anorthite precipitated according to the sol–gel route, T5, the microstructural result is different. Here, too, the macroscopic structure seems almost unchanged before and after the experiment. However, a detailed examination after the test shows that wollastonite has formed inside the anorthite, which can be seen in the measurements in Figure 9.

4 | DISCUSSION

Already the macroscopic observation (Figure 2) showed visible differences between the samples after the particular experiments, which is more pronounced at higher temperatures. The mass control of the samples showed a small but reproducible loss. This corresponds well with the results of

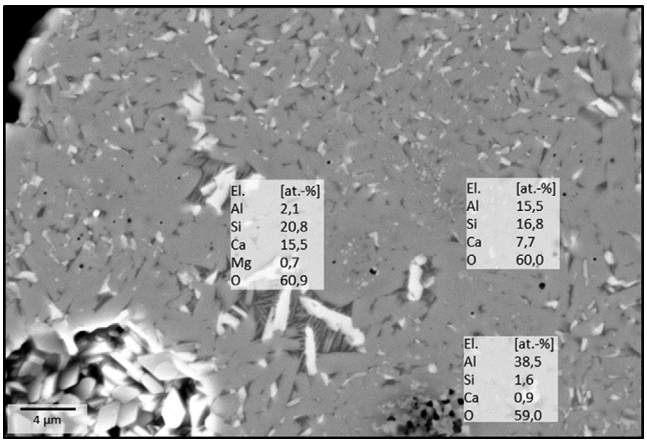

FIGURE 9 SEM micrograph of anorthite, based on sol, after T5 (1100°C 24 h)

the XRF. A mass regain due to oxidation observable as well as a loss of phosphor. The removal of phosphor from the castable is easily explainable by the reduction of diphosphorpentaoxide into less oxidized variants like phosphortrioxide, which evaporates due to its low vapor pressure under the given conditions of the 9 Ar 1 H_2 atmosphere. The gaseous phosphorus oxides are then carried out of the system with the general direction of the gas flow or, as later shown, build up into the iron agglomerates.

Changes in the mineral phases of the bauxite castable could not be detected by means of XRD, as the relative intensities of the main phases are too predominant. An analysis of the sample surface would possibly have shown a local phase change, which could be observed later using the SEM.

It becomes clear that the surfaces are changed by the growth of layers. Less oxygen affine elements, such as iron and phosphor, are transported from the sample interior to the sample surface as well as into the pore volume. Here these elements then form agglomerates and in case of the outer sample surface start the formation of a layer. The samples are permeated by the hydrogen due to its high fugacity. This leads to the reduction of impurities, such as iron oxide, phosphor oxide, and titanium oxide, and therefore enhances their moveability. These then follow the concentration gradient to the interface of the surrounding gas and the sample itself. The fact that these layers lose their metallic character is due to the reoxidation during the cooling process in the test set-up. These observations are clear for the conditions of experiment T2 but were not evident for the T1 conditions. The increase in duration for T3 shows the formation of an additional layer, consisting out of titanium oxide, which has a similar oxygen affinity as silica. The reactions and the movement of the impurities in the bauxite castable have been observed.

In general, silica containing refractory components such as anorthite and mullite should be reduced. In these examinations, the reduction reaction for iron oxide, phosphor oxide, and titanium oxide is evident. An expectable decomposition of the main refractory components is not taking place in these studies XRD as well as SEM/EDS obersavtions confirm this correspondingly. The accompanying elements iron oxide, phosphor oxide, and titanium oxide react first, as they have a lower affinity for oxygen.

It was already clear from the phase determination that changes occur in the matrix phase. In both series of the experiments T4 and T5, the decomposition of the anorthite is only beginning, which can be explained by the conditions of the experiment: only 10 % of the gas is reaction-generating hydrogen. Interesting here is the tendency of the two formulations to behave differently. T4, anorthite 1, mainly decomposes into CA_6 at fine fringes of the material. In case of T5, anorthite 2, we can observe the formation of wollastonite in the bulk of the material.

5 | CONCLUSION

It becomes clear that the permeation of the porous castable sample with H_2 takes place, which leads to the reduction of the less oxygen affine compounds, that is, iron and titanium oxides. These have an increased mobility due to the reduction and move toward the surface of the sample according to the concentration gradient of the entire system.

The reduction and corresponding partial removal via the gas flow of the phosphor oxides could be detected. While chemical composition, determined by XRF, gives no indication of a significant loss of iron and titanium, it shows clear signs of the loss of the phosphor, which forms gaseous compounds under the given conditions.

However, these impurity reactions may overlay possible reactions and decomposition occurring in the binding phase itself. Thus, no mineralogical changes could be detected. Isolating these phases using the example of anorthite, resulting reaction can be determined. Due to the decomposition of anorthite, CA_6 and wollastonite could be observed. This was possible despite the reduced temperature from 1500°C to 1100°C and should be more pronounced at higher temperatures.

ORCID

T. Leber https://orcid.org/0000-0002-0342-0401

REFERENCES

1. Hölling M, Wenig M, Gellert S. Bewertung der Herstellung von Eisenschwamm unter Verwendung von Wasserstoff. News und Pressemitteilungen ArcelorMittal Hamburg GmbH, 2017.

2. Vogl V, Ahman M, Nilsson LJ. Assessment of hydrogen direct reduction for fossil-free steelmaking. J Cleaner Prod. 2018;203:736–45.
3. Tso ST, Pask JA. Reaction of silicate glasses and mullite with hydrogen gas. J Am Ceram Soc. 1982;65:383–7.
4. Tai W-P, Watanabe T, Jacobson NS. High-temperature stability of alumina in argon and argon/water-vapor environments. J Am Ceram Soc. 1999;82:245–8.
5. Opila EJ, Myers DL. Alumina volatility in water vapor at elevated temperatures. J Am Ceram Soc. 2004;87:1701–5
6. Gentile PS, Sofie SW, Key CF, Smith RJ. Silicon volatility from alumina and aluminosilicates under solid oxide fuel cell operating conditions. Int J Appl Ceram Technol. 2012;9:1035–48.
7. Takeuchi N, Shiomi S, Ohba Y. Thermal changes of mullite based castable heated in hydrogen atmosphere. In: Unified International Technical Conference of Refractories, Yokohama, Japan; 2019.
8. Ellingham JT. Reducibilty of oxides and sulphides in metallurgical processes. J Appl Chem Biotechnol. 1944;63(5): 125–60.
9. Selly RC, Cocks R, Pilmer I. Encyclopedia of geology (Vol. 5). Elsevier Academic, ISBN 0126363838 S. S.32ff 2005.
10. Shackelford J, Doremus R. Ceramic and glass materials—structure, properties and processing. Springer, ISBN 978-0-387-73361-6 S.41ff 2008.

How to cite this article: Leber T, Madeo S, Tonnesen T, Telle R. Corrosion of bauxite-based refractory castables and matrix components in hydrogen containing atmosphere. Int J Ceramic Eng Sci. 2022;4:16–22.
https://doi.org/10.1002/ces2.10111